HHS Public Access

Author manuscript

Science. Author manuscript; available in PMC 2019 September 01.

Published in final edited form as:

Science. 2019 March 01; 363(6430): 989–993. doi:10.1126/science.aaw2586.

A lipase-independent pathway of lipid release and immune modulation by adipocytes

Stephen E Flaherty III[1,†], **Ambar Grijalva**[1,†], **Xaioyuan Xu**[1], **Eleanore Ables**[1], **Alireza Nomani**[2], and **Anthony Ferrante Jr.**[1,*]

[1]Department of Medicine, Naomi Berrie Diabetes Center, Columbia University, New York, NY 07043, USA

[2]Department of Pharmaceutics, Rutgers University, Piscataway, NJ 08854, USA

Abstract

To meet systemic metabolic needs, adipocytes release fatty acids and glycerol through the action of neutral lipases. Here we describe a secondary pathway of lipid release from adipocytes that is independent of canonical lipolysis. We found that adipocytes release exosome-sized, lipid-filled vesicles (AdExos) that become a source of lipid for local macrophages. Adipose tissue from lean mice released ~ 1% of its lipid content per day via exosomes ex vivo, a rate that more than doubles with obesity. AdExos and associated factors were sufficient to induce in vitro differentiation of bone marrow precursors into adipose tissue macrophage-like cells. Thus, AdExos are both an alternative pathway of local lipid release and a mechanism by which parenchymal cells can modulate tissue macrophage differentiation and function.

In most terrestrial animals, adipocytes serve as key energy storage cells, containing large, unilocular droplets of triacylglyceride (TAG) and other neutral lipids. Hydrolysis of adipocyte TAG supplies substrates to meet systemic metabolic needs during periods of negative energy balance (1); however, in the setting of obesity and other metabolic disorders, excess lipid accumulates in cells of other tissues including liver, skeletal muscle and heart (2). Locally within adipose tissue, lipids also regulate immune cells, in particular adipose tissue macrophages (ATMs), the predominant immune cell in fat (3) (4). In ATMs, accumulation of neutral lipid activates a program of lysosomal catabolism, a process that is essential for TAG hydrolysis and that is associated with systemic metabolic complications including insulin resistance and hepatic steatosis (5). We previously hypothesized that the neutral lipid within ATMs is generated from adipocyte-derived fatty acids that are re-esterified and incorporated in lipid droplets by ATMs. Our recent studies, however, suggest that lipid catabolism in ATM lysosomes occurs by a mechanism that is independent of autophagy (6). Given that autophagy is thought to be essential for lipid delivery from lipid

*Corresponding author. awf7@columbia.edu.

†Contributed Equally

Author Contributions: A.W.F. and S.E.F. developed the research strategy and experimental designs; S.E.F., A.G., E.A., X.X., A.N. performed the experiments; A.W.F. coordinated all activities, A.W.F and S.E.F. prepared the figures and wrote the manuscript. All authors approved the final manuscript.

Competing interests: Authors declare no competing interests.

Data and Material Availability: All data are available in the manuscript or the supplementary material.

droplets to lysosomes, an autophagy-independent mechanism in ATMs suggests that lipid destined for lysosomal catabolism may not be contained within lipid droplets (6).

To determine whether lipid in ATMs is localized within lipid droplets, we analyzed the expression of lipid droplet protein Perilipin 2 in primary ATMs. Perilipins and related PAT family proteins associate with the phospholipid layer that covers lipid droplets (7). In previous analyses and consistent with data on other macrophages, we found *Perilipin 2 (Plin2*) is the predominate PAT gene expressed in ATMs (5). Confocal fluorescence microscopy of adipose tissue, however, revealed that most lipid in ATMs does not co-localize with Perilipin 2 (Fig. 1A). This is in contrast to findings with foam cells – the cholesterol-laden macrophages of atherosclerotic plaques – in which a substantial portion of neutral lipid is located in lipid droplets and undergoes autophagy (8). By transmission electron microscopy, autophagolysosomes are readily apparent in foam cells, but no such structures were visible in ATMs (Fig. 1B). Lipid in ATMs appears to be stored in vesicles, distinct from the lipid droplets seen in foam cells. Given that lipid droplets form in the endoplasmic reticulum during TAG synthesis from fatty acids and glycerol, these findings suggest that accumulation of neutral lipid may not occur through a re-esterification of free fatty acids. One possible mechanism of lipid accumulation is through endocytic uptake of intact neutral lipid.

Bone-marrow cells differentiated in the presence of adipose tissue (BM-ATMs) exhibit an ATM-like phenotype with morphologic and functional characteristics typical of primary ATMs, including neutral lipid accumulation, multinuclear formation, a transcriptional profile characteristic of ATMs, lysosome biogenesis and lipid catabolism (5, 6). The ability of adipose tissue to drive bone marrow cells to an ATM phenotype mirrors the ability of osteoblasts to induce osteoclast differentiation and permits analysis of factors involved in ATM development and transfer of lipid from adipocytes to macrophages. The canonical release of lipid from adipocytes requires the action of a series of neutral lipases, of which Adipose triglyceride lipase/Desnutrin/Patatin-like phospholipase domain-containing protein 2 (ATGL) catalyzes the initial step (9, 10). To investigate whether the canonical pathway is required for lipid accumulation in ATMs, we differentiated bone marrow cells into macrophages in the presence of adipose tissue from wild-type mice or from mutant mice deficient in ATGL (*Atgl/Pnpla2*$^{-/-}$) (Fig. 1C). We also examined the ability of wild-type mouse adipose tissue that had been treated with an ATGL inhibitor to cause lipid accumulation in BM-ATMs (Fig. 1D). Consistent with a non-hydrolytic release of lipids, we found that the accumulation of neutral lipids in ATMs does not require adipocyte ATGL.

We next examined images of whole adipose tissue to discern whether there were any structures that might indicate the release of intact neutral lipid from adipocytes. Electron micrographs (EMs) revealed that invaginated lipid structures, consistent with the fusion or budding of smaller lipid droplets, are associated with the central lipid droplet of adipocytes (Fig. 2A). In addition, these vesicles were near structures reminiscent of multivesicular endosomes (Fig. 2A), structures typically involved in the biogenesis and release of extracellular vesicles (12). Together these images and the data from ATMs prompted us to consider whether adipocytes release lipid-containing extracellular vesicles that enter an endocytic pathway in ATMs. To determine whether such adipocyte-derived vesicles exist,

we cultured mouse perigonadal adipose tissue (PGAT) in the absence of serum and analyzed the conditioned medium for extracellular vesicles. EMs of adipose tissue-conditioned medium revealed the presence of a high concentration of extracellular vesicular particles ranging in diameter from 50 to 100nm, consistent with the size of exosomes and related extracellular vesicles (Fig. 2B). Standard purification strategies for exosomes proved inefficient, possibly because of high lipid content; however, using size fractionation columns and filtration, we were able to isolate extracellular vesicles from adipose tissue. The particles contained canonical exosomal proteins (Fig. 2C), as well as adipocyte-specific proteins (Fig. 2D and fig. S1). If the invaginations seen in EM images represent budding (Fig. 2A), we predicted that any adipocyte-derived exosome would contain a lipid droplet and its associated proteins, including ATGL and PLIN1 (Fig. 2E). Consistent with this prediction, both ATGL and PLIN1 were detected in exosomes. Analysis of adipose tissue from which ATGL had been specifically deleted in adipocytes, confirmed the adipocyte origin of the exosomal ATGL (fig. S2). We also confirmed the predicted topology of the exosomes (Fig. 2E) using proteinase digestion: the lipid-droplet-associated protein ATGL was resistant to proteinase digestion, whereas the cytoplasmic membrane derived protein CD63 was susceptible (Fig. 2F).

Combining laser light scattering microscopy with a charge-coupled device (CCD) camera enables nanoparticle detection resulting in accurate vesicle quantification and size estimation (13). Consistent with our EM images, nanoparticle tracking analysis of adipose-derived exosomes from lean C57BL/6J mice revealed that they had a mean diameter of 118 +/− 57 nm (median 102 nm). Exosomes isolated from leptin-deficient ($Lep^{ob/ob}$) obese mice had a mean diameter of 115 +/− 54 nm (median 104 nm) that was indistinguishable from those of lean adipose tissue (Fig. 2I). PKH26 is a fluorescent dye that intercalates within phospholipid bilayers and labels exosomes. When added to adipose tissue-conditioned medium, PKH26 fluorescence copurified with exosomes as measured using nanoparticle detection (fig. S3A). In ex vivo experiments, PGAT from lean mice released on average 1.3×10^{11} exosomes per gram of tissue per hour, whereas PGAT from obese ($Lep^{ob/ob}$) mice released 3.5×10^{11} exosomes/g/hr (Fig. 2G). Roughly 6.0×10^{11} exosomes were released from obese tissue every 2 hours, a rate that remained constant through 12 hours in culture (fig. S3B). The number of exosomes released from adipose tissue is also acutely modulated *in vivo*; PGAT from fasted mice released exosomes at a rate more than twice that of adipose tissue from fed animals (fig. S4).

To confirm the adipocyte origin of these exosomes and track them *in vivo* we created a mouse line that expresses the fluorescent protein tdTomato specifically in adipocytes (AdTom) (fig. S5). Exosomes isolated from adipose tissue of these mice were fluorescent (fig. S6) and contained the tdTomato protein (Fig. 3A). The fluorescence of exosomes released from whole adipose tissue was comparable to that of exosomes released from purified AdTom adipocytes, consistent with majority of exosomes released from adipose tissue being adipocyte-derived (Fig. 3B). Adipocyte-derived exosomes were readily detected in the blood of AdTom mice but the ratio of CD63 to dtTomato suggested that they represent a minority of the exosomes in the circulation (Fig. 3C). This is in contrast to a recent report that the majority of circulating exosomes are adipocyte-derived (13).

The homogenous appearance of the centers of AdExos in electron micrographs and the presence of lipid-droplet-associated proteins suggested that AdExos contain neutral lipid. Isolated AdExos contain little free fatty acid as compared to the total amount released from PGAT (fig. S7). In contrast, 400mg of PGAT from a lean mouse released 980 nmol of acylglycerides per hour in exosomes (Fig. 3D), the equivalent of ~0.04% of the total acylglyceride content of the fat pad (Fig. 3E). In obese (*Lep*$^{ob/ob}$) mice the rate of lipid release increases to ~0.1% of total adipocyte acylglycerides per hour. While these rates are dwarfed by the release of lipid during maximally activated lipolysis, a steady release rate implies the complete turnover of lipid within adipocytes every 104 days in lean animals and every 42 days in obese animals (Fig. 3E). Inhibition of lipolysis with an ATGL inhibitor reduced FFA release from adipose tissue but did not affect AdExo release (fig. S8). Through targeted lipidomics we found, in addition to phospholipids and free cholesterol that would be expected as part of both the lipid droplet and cytoplasmic membrane components of AdExos, that adipocyte-derived exosomes contain stoichiometrically large amounts of tri- and mono-acylglycerides (fig. S9). Based on physical chemical properties and the concentration of mono-and tri-acylglycerides, we would predict a volume of 2.6×10^{-21} m^3 of acyl-glyceride per exosome. This is roughly consistent with predicted internal volume of AdExos (based on measured exosome diameter) of between 1.5×10^{-21} and 7.2×10^{-21} m^3.

Lipid accumulates in ATMs with increasing adiposity (5) and accumulates in bone marrow cells *in vitro* when they are differentiated in the presence of adipose tissue (Fig. 1). To determine whether AdExos are taken up directly by ATMs within intact adipose tissue, we labeled AdExos with the fluorescent dye PKH26 and injected them into PGAT depots of lean C57BL/6J mice. Adipocytes and stromal vascular cells (SVCs) were collected from PGAT 16 hours after injection, lysed, and measured for PKH26 fluorescence. The PKH26 label was found to localize exclusively to the SVC fraction of the PGAT (Fig. 4A). This SVC fraction was further analyzed using flow cytometry, and exosome uptake was found almost exclusively (~90%) in F4/80+ macrophages (Fig. 4B and fig. S10). These data demonstrate that adipocyte-released exosomes are taken up by ATMs in intact adipose tissue in vivo. Ex vivo conditioned medium of adipose tissue and CSF-1 cause lipid accumulation and differentiation of bone marrow cells into ATM-like cells. AdExos were sufficient to cause lipid accumulation in CSF-1-treated bone marrow cells (Fig. 4C, 4D). Lipidomics analysis of these BM-ATMs revealed that AdExos specifically increased the TAG content of ATMs, eightfold, compared to bone marrow-derived macrophages (BMDMs) not provided AdExos (Fig. 4C). Consistent with the uptake of intact TAGs, the lipid content of BM-ATMs is not dependent on fatty acid esterification via diglyceride acyltransferase 1 & 2 (DGAT1 and DGAT2) (fig. S11), but lipid uptake is blocked by LY294002 (Fig. 4E) a PI3K inhibitor that prevents macropinocytosis but does not interfere with micropinocytosis or DGAT activity.

The adipose tissue conditioned medium from which we purify AdExos not only leads to lipid accumulation in macrophages, but also induces differentiation of bone marrow progenitors into ATM-like cells, causing lysosome biogenesis and activating a transcriptional program that is characteristic of ATMs (5). To determine whether AdExos contribute to ATM differentiation, we treated mouse bone marrow cells with CSF-1 for three days, followed by treatment with CSF-1 and AdExos for an additional six days. Cells treated

with AdExos accumulated lipid, became multinucleated, and displayed an increase in lysosomal content, defining features of ATMs (Fig. 4F and fig. S12). AdExos also progressively activated a transcriptional profile characteristic of ATMs, including a subset of genes previously identified as distinguishing ATMs from other tissue-resident macrophage populations (*Cxcl1, Tnfsf9*), but not genes associated with other tissue-resident macrophage populations, e.g. Kupffer cells (*Marco, Dampk*) (Fig. 4G and fig. S13). The effects of AdExos on differentiation are not a general effect of exosomes, given that exosomes from primary osteoblasts did not induce the same expression profile. Among genes involved in lipid metabolism, AdExos induced the expression of intracellular lipid binding protein gene *Fabp4* but had no effect on the expression of the fatty acid transporter *Cd36,* whereas treatment with the filtrate (fatty-acid-containing) fraction did increase *Cd36* expression in BMDMs, consistent with the disparate effects of FFA and AdExos on BMDM differentiation.

Adipocyte-derived exosomes have been described previously – primarily as regulators of inflammation and systemic insulin resistance (13–18). However, given the lipid content of the AdExos described here, it is unclear whether previous studies using standard protocols to isolate exosomes would have missed these AdExos. Here we found that adipocytes release lipid-laden exosomes that deliver TAG locally to macrophages and drive their differentiation. While the systemic release of free fatty acids by adipocytes is part of a well-established cycle of substrate storage and release (19) (20), the evidence for release of TAG by adipocytes has been scant. Locally, this pool of TAG is taken up and hydrolyzed by ATMs, establishing a local lipid cycle. The atrophy of fat depots in mice lacking the ability of ATMs to hydrolyze TAG in endolysosomes (21) suggests that this cycle may be important to maintain adipose tissue homeostasis. The detection of AdExos in the circulation of mice provides a possible, previously unrecognized source of plasma triglycerides; the size and significance of this pool remains to be determined.

Regulation of the tissue specific phenotypes and functions of macrophages is not well understood. CSF-1 (and in some cases Il-34 and CSF-3/GM-CSF) is a key regulator of differentiation of most macrophage populations (22), but clearly other signals must direct the tissue specific development and phenotype of cells. In bone, osteoblasts are known to elaborate TNFSF11/RANKL that, with CSF-1, induces differentiation of osteoclasts (bone macrophages) (23). However, few other examples exist where local factor(s) that drive tissue-specific differentiation of macrophages are known. Adipocyte-derived exosomes appear to play that function in fat and offer the possibility that a similar process may occur in other tissues. This would suggest that cellular machinery associated with the endolysosomal pathway can sense the content of exosomes and drive differentiation of macrophages to adapt and meet the needs of their local microenvironment.

Supplementary Material

Refer to Web version on PubMed Central for supplementary material.

ACKNOWLEDGMENTS:

We thank E. Kershaw for Atgl-floxed mice, and K. Brown, R. Chan, G. Di Paolo, P. Petropoulou, S. Kousteni, H. Ginsberg, S. Ramakrishan and A.Hatefi for technical assistance and advice.

Funding: NIH grants R01DK066525, P30DK026687, P30DK063608, T32DK007328 and support from the Russell Berrie Foundation.

References and Notes:

1. Scherer PE, Adipose tissue: from lipid storage compartment to endocrine organ. Diabetes 55, 1537–1545 (2006). [PubMed: 16731815]
2. Shulman GI, Ectopic fat in insulin resistance, dyslipidemia, and cardiometabolic disease. N Engl J Med 371, 1131–1141 (2014). [PubMed: 25229917]
3. Kosteli A, Sugaru E, Haemmerle G, Martin JF, Lei J, Zechner RFerrante AW Jr, Weight loss and lipolysis promote a dynamic immune response in murine adipose tissue. J Clin Invest 120, 3466–3479 (2010). [PubMed: 20877011]
4. Mottillo EP, Shen XJ, Granneman JG, Role of hormone-sensitive lipase in beta-adrenergic remodeling of white adipose tissue. Am J Physiol Endocrinol Metab 293, E1188–1197 (2007). [PubMed: 17711991]
5. Xu X, Grijalva A, Skowronski A, van Eijk M, Serlie MJ, Ferrante AW Jr. Obesity activates a program of lysosomal-dependent lipid metabolism in adipose tissue macrophages independently of classic activation. Cell Metab 18, 816–830 (2013). [PubMed: 24315368]
6. Grijalva A, Xu X, Ferrante AW Jr., Autophagy Is Dispensable for Macrophage-Mediated Lipid Homeostasis in Adipose Tissue. Diabetes 65, 967–980 (2016). [PubMed: 26868294]
7. Kimmel AR, Sztalryd C, The Perilipins: Major Cytosolic Lipid Droplet-Associated Proteins and Their Roles in Cellular Lipid Storage, Mobilization, and Systemic Homeostasis. Annu Rev Nutr 36, 471–509 (2016). [PubMed: 27431369]
8. Ouimet M, Franklin V, Mak E, Liao X, Tabas I, Marcel YL. Autophagy regulates cholesterol efflux from macrophage foam cells via lysosomal acid lipase. Cell Metab 13, 655–667 (2011). [PubMed: 21641547]
9. Villena JA, Roy S, Sarkadi-Nagy E, Kim KH, Sul HS, Desnutrin, an adipocyte gene encoding a novel patatin domain-containing protein, is induced by fasting and glucocorticoids: ectopic expression of desnutrin increases triglyceride hydrolysis. J Biol Chem 279, 47066–47075 (2004). [PubMed: 15337759]
10. Zechner R, Kienesberger PC, Haemmerle G, Zimmermann R, Lass A, Adipose triglyceride lipase and the lipolytic catabolism of cellular fat stores. J Lipid Res 50, 3–21 (2009). [PubMed: 18952573]
11. Raposo G, Stoorvogel W, Extracellular vesicles: exosomes, microvesicles, and friends. J Cell Biol 200, 373–383 (2013). [PubMed: 23420871]
12. Filipe V, Hawe A, Jiskoot W, Critical evaluation of Nanoparticle Tracking Analysis (NTA) by NanoSight for the measurement of nanoparticles and protein aggregates. Pharm Res 27, 796–810 (2010). [PubMed: 20204471]
13. Thomou T, Mori MA, Dreyfuss JM, Konishi M, Sakaguchi M, Wolfrum C, Rao TN, Winnay JN, Garcia-Martin R, Grinspoon SK, Gorden P, Kahn CR, Adipose-derived circulating miRNAs regulate gene expression in other tissues. Nature 542, 450–455 (2017). [PubMed: 28199304]
14. Deng ZB, Poliakov A, Hardy RW, Clements R, Liu C, Liu Y, Wang J, Xiang X, Zhang S, Zhuang X, Shah SV, Sun D, Michalek S, Grizzle WE, Garvey T, Mobley J, Zhang HG, Adipose tissue exosome-like vesicles mediate activation of macrophage-induced insulin resistance. Diabetes 58, 2498–2505 (2009). [PubMed: 19675137]
15. Dai M, Yu M, Zhang Y, Tian W, Exosome-Like Vesicles Derived from Adipose Tissue Provide Biochemical Cues for Adipose Tissue Regeneration. Tissue Eng Part A, (2017).
16. Koeck ES, Iordanskaia T, Sevilla S, Ferrante SC, Hubai MJ, Freishtat RJ, Nadier EP, Adipocyte exosomes induce transforming growth factor beta pathway dysregulation in hepatocytes: a novel paradigm for obesity-related liver disease. J Surg Res 192, 268–275 (2014). [PubMed: 25086727]

17. Zhang Y, Yu M, Tian W, Physiological and pathological impact of exosomes of adipose tissue. Cell Prolif 49, 3–13 (2016). [PubMed: 26776755]

18. Crewe C, Joffin N, Rutkowski JM, Kim M, Zhang F, Towler DA, Gordilo R, Scherer PE, An Endothelial-to-Adipocyte Extracellular Vesicle Axis Governed by Metabolic State. Cell, 175, 695–708 (2018). [PubMed: 30293865]

19. Storlien L, Oakes ND, Kelley DE, Metabolic flexibility. Proc Nutr Soc 63, 363–368 (2004). [PubMed: 15294056]

20. Nielsen TS, Jessen N, Jorgensen JO, Moller N, Lund S, Dissecting adipose tissue lipolysis: molecular regulation and implications for metabolic disease. J Mol Endocrinol 52, R199–222 (2014). [PubMed: 24577718]

21. Du H, Heur M, Duanmu M, Grabowski GA, Hui DY, Witte DP, Mishra J, Lysosomal acid lipase-deficient mice: depletion of white and brown fat, severe hepatosplenomegaly, and shortened life span. J Lipid Res 42, 489–500 (2001). [PubMed: 11290820]

22. Stanley ER, Chitu V, CSF-1 receptor signaling in myeloid cells. Cold Spring Harb Perspect Biol 6, (2014).

23. Yasuda H, Shima N, Nakagawa N, Yamaguchi K, Kinosaki M, Mochizuki S, Tomoyasu A, Yano K, Goto M, Murakami A, Tsuda E, Morinaga T, Higashio K, Udagawa N, Takahashi N, Suda T, Osteoclast differentiation factor is a ligand for osteoprotegerin/osteoclastogenesis-inhibitory factor and is identical to TRANCE/RANKL. Proc Natl Acad Sci U S A 95, 3597–3602 (1998). [PubMed: 9520411]

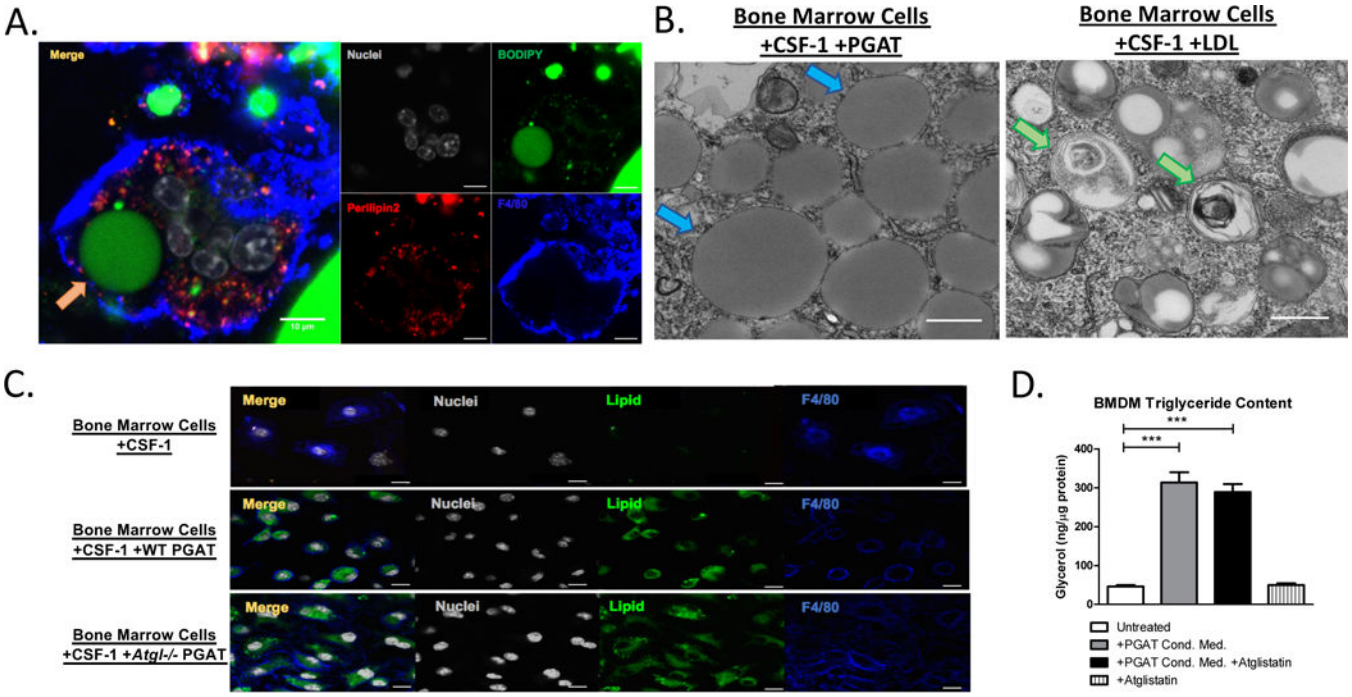

Figure 1. Lipid accumulates in adipose tissue macrophage lipid vesicles, independently of adipocyte ATGL lipase activity.

(A) Confocal microscopy images of whole perigonadal adipose tissue from *Lep ob/ob* mice, immunostained with antibodies against Perilipin2 (Red) and F4/80 (Blue) and incubated with DNA fluorescent stain DAPI (White) and neutral lipid fluorescent stain BODIPY (Green). Arrow highlights lipid accumulation within ATM (Orange Arrow). Scale bars represent 10µm. **(B)** Electron microscopy images of bone marrow-derived adipose tissue macrophages (BM-ATMs) (left) and bone marrow-derived foam cells (right). Arrows highlight lipid vesicles (Blue) and lipid-rich autophagosomes (Green). Scale bars represent 200nm. **(C)** Confocal microscopy images of bone marrow-derived macrophages (BMDMs) (top), BM-ATMs differentiated in the presence of adipose tissue (middle), or BM-ATMs differentiated in the presence of *Atgl/Pnpla2*-deficient adipose tissue (bottom), immunostained with antibodies against F4/80 (Blue), as well as DNA fluorescent stain DAPI (White) and neutral lipid fluorescent stain BODIPY (Green). Scale bars represent 10µm. **(D)** Triglyceride content of BMDMs (untreated) or treated with medium containing Atglistatin, BM-ATM differentiated with condition medium of wild-type perigonadal adipose tissue, or with conditioned medium wild-type perigonadal adipose tissue treated with 50µM Atglistatin (One-way ANOVA. n = 6; *** p-value < 0.001).

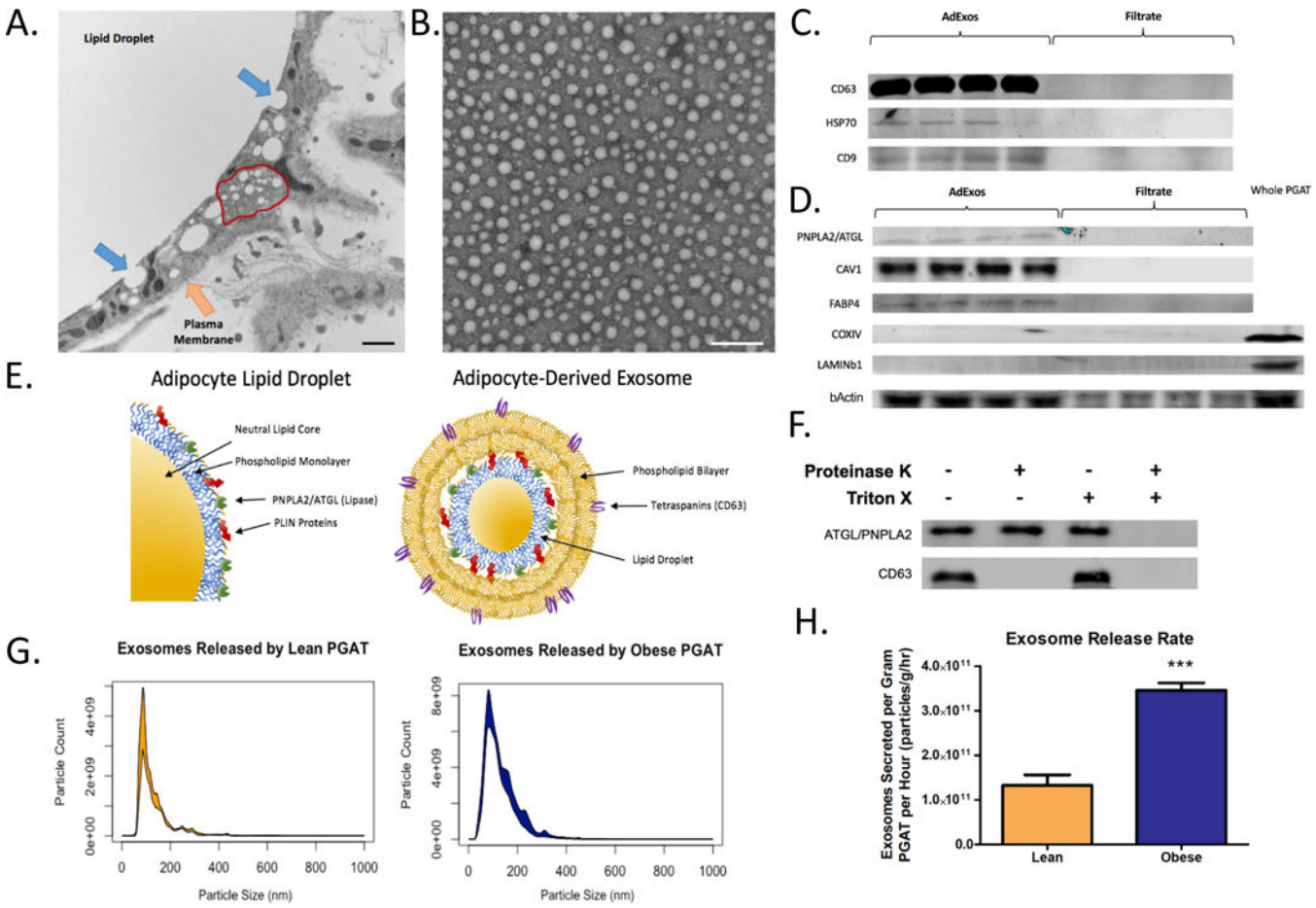

Figure 2. Obese Adipocytes Release More Exosomes than Lean Adipocytes.

(A) Electron microscopy image of whole, fixed adipose tissue. Arrows highlight the adipocyte plasma membrane (Orange Arrow), the budding-like structures of the central lipid droplet (Blue Arrow), and a multivesicular endosome-like structure (Red Outline). Scale bar represents 200nm. **(B)** Electron microscopy image of vesicles collected from adipose tissue conditioned medium. Scale bar represents 200nm. **(C)** Western blots of exosomal protein isolated from adipose tissue conditioned media (Ad-Exosomes), and conditioned media content smaller than 100kD (Filtrate). Blots were probed using antibodies against CD63, HSP70, and CD9. **(D)** Western blots of exosomal protein isolated from adipose tissue conditioned media (Ad-Exosomes), conditioned media content smaller than 100kD (Filtrate), and whole perigonadal adipose tissue (Whole PGAT). Blots were probed using antibodies against ATGL, CAV1, FABP4, COXIV, Lamin B1, and b-Actin. **(E)** Graphical representation of adipocyte lipid droplet structure (left) and hypothesized structure of adipocyte-derived exosome (right). **(F)** Western blots of protein extracted from purified exosomes that were untreated, treated with 100μg/mL Proteinase K, treated with 0.5% Triton-X100, or both. Blots were probed with antibodies against CD63 and ATGL. **(G)** Nanoparticle Tracking Analysis histogram of purified adipose-derived exosomes, depicting particle diameter, and the number of particles at each diameter released by one gram of lean (left, red) or leptin-deficient (*Lep*$^{ob/ob}$) obese (right, blue) adipose tissue per hour. **(H)**

Quantification of exosome released by adipose tissue per gram per hour from adipose tissue from lean and ($Lep^{ob/ob}$) obese mice (Unpaired two-tailed t-test. n = 8; *** p-value < 0.001).

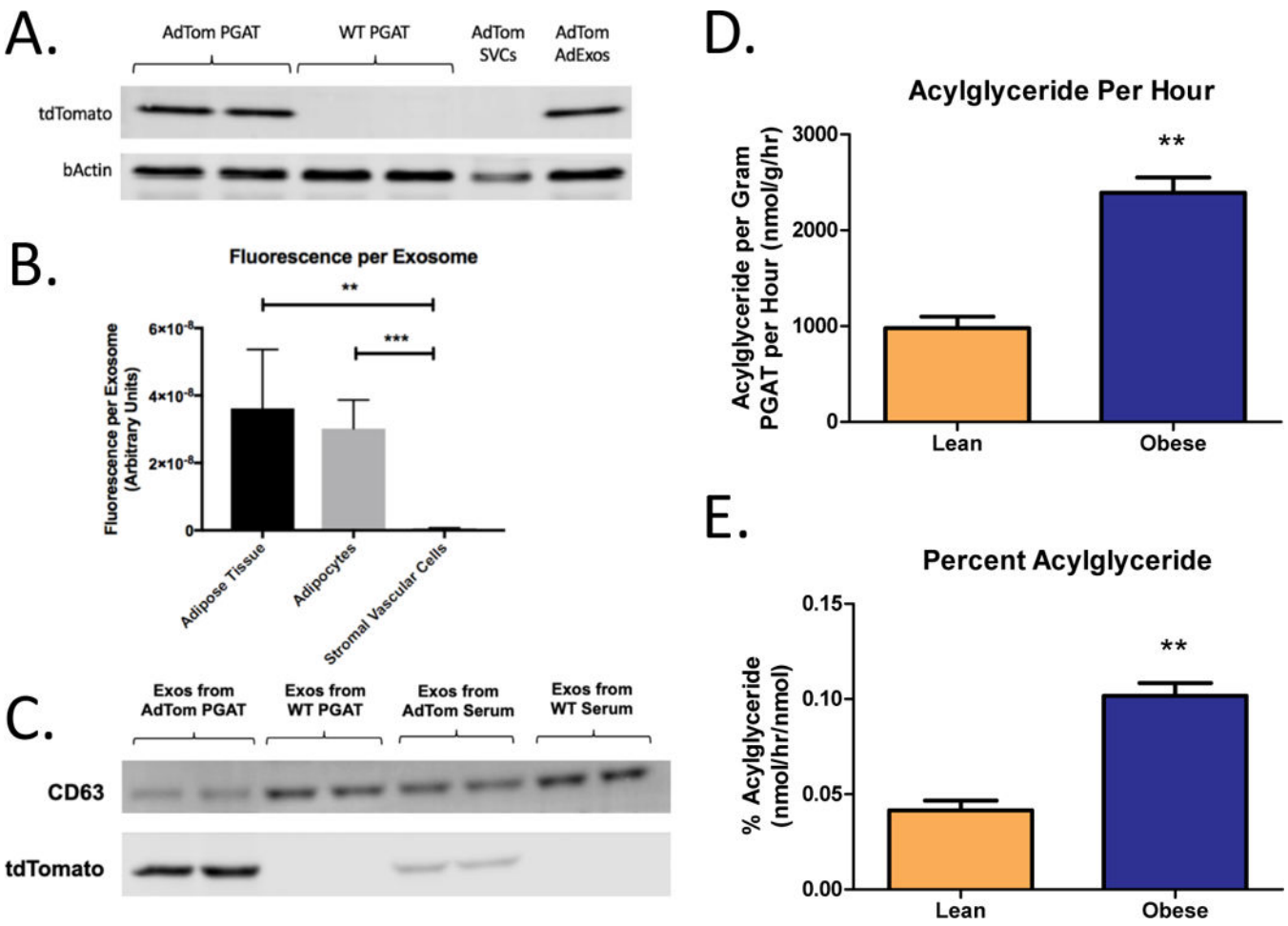

Figure 3. Adipocyte derived exosomes transport neutral lipid.

(A) Western blot of total protein from whole AdTom PGAT, WT PGAT, SVCs isolated from AdTom PGAT, and AdExos isolated from AdTom PGAT. Blots were probed using antibodies against tdTomato and bActin. **(B)** TdTomato fluorescence per exosome, as measured by Nanoparticle Tracking Analysis, for AdExos purified from whole AdTom PGAT, adipocytes isolated from AdTom PGAT, and SVCs isolated from AdTom PGAT (One-way ANOVA. n = 4, ** p-value < 0.01, *** p-value < 0.001). **(C)** Western blot of total protein from AdExos isolated from AdTom PGAT, AdExos isolated from WT PGAT, exosomes isolated from AdTom serum, and exosomes isolated from WT serum. Blots were probed using antibodies against CD63 and tdTomato. **(D)** Acylglyceride content of purified adipocyte-derived exosomes from lean and obese (*Lep*$^{ob/ob}$) adipose tissue per gram of PGAT per hour (Unpaired two-tailed t-test. n = 8; ** p-value < 0.01). **(E)** Acylglyceride content of purified adipocyte-derived exosomes, expressed as a percentage of the acylglyceride content of the tissue itself (Unpaired two-tailed t-test. n = 8; ** p-value < 0.01).

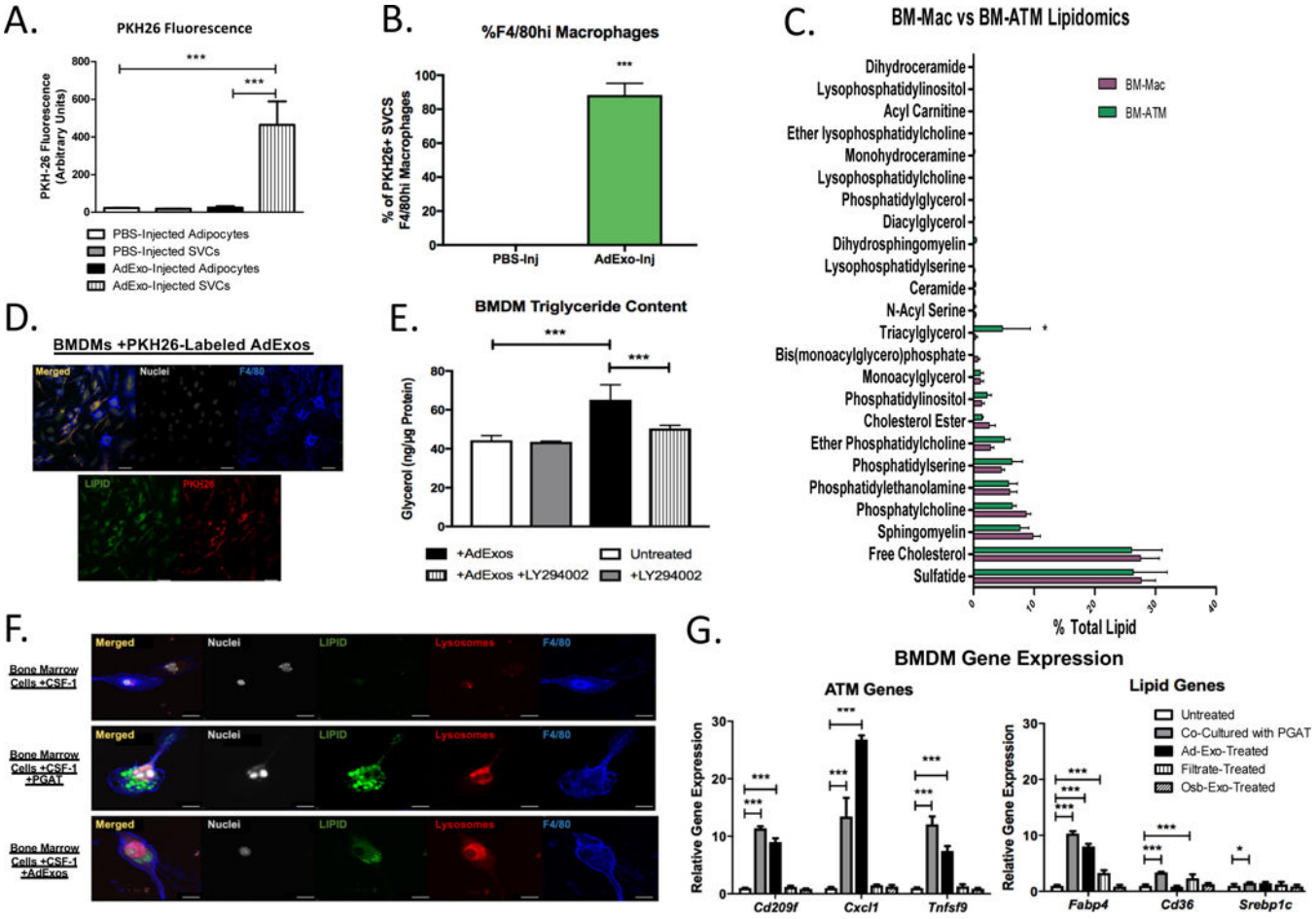

Figure 4. AdExos are taken up by macrophages and induce an ATM-like phenotype in bone marrow cells.

(A) PKH26 Fluorescence of adipocyte and SVC lysates from PGAT injected with PBS (left) or PKH26-labeled AdExos (right) (one-way ANOVA. n = 4; *** p-value < 0.001). **(B)** Percent PKH26+ SVCs that are CD45.2+,CD11b+,F4/80hi macrophages is quantified for PBS-Inj and AdExo-Inj groups (right) (Unpaired two-tailed t-test. n = 4; *** p-value < 0.001). **(C)** Targeted lipidomics of bone marrow-derived macrophages cultured with (BM-ATM) or without (BM-Mac) the presence of adipose tissue (Unpaired two-tailed t-test. n=3; * p-value < 0.05). **(D)** Confocal microscopy images of *in vitro*-generated bone-marrow-derived macrophages cultured with PKH26-labeled AdExos and immunostained with antibodies against F4/80 (Blue), as well as DNA fluorescent stain DAPI (White) and neutral lipid fluorescent stain BODIPY (Green). Scale bars represent 10µm. **(E)** Triglyceride levels of BMDMs cultured alone, with 100µM LY294002, with AdExos, or with both 100µM LY294002 and AdExos for 24 hours, measured enzymatically (One-way ANOVA. n = 6; *** p-value < 0.001). **(F)** Confocal microscopy images of *in vitro*-generated bone-marrow-derived macrophages either cultured alone (top), with wild-type perigonadal adipose tissue (second from top), or with AdExos (bottom) for 3 days, immunostained with antibodies against F4/80 (Blue), as well as DNA fluorescent stain DAPI (White), neutral lipid fluorescent stain BODIPY (Green), and acidic organelle stain Lysotracker (Red). Scale bars

represent 10μm. **(G)** Quantitative PCR for bone-marrow-derived macrophages cultured alone, with wild-type perigonadal adipose tissue, with AdExos, with filtrate from PGAT conditioned medium (AdExos removed), or with exosomes secreted from primary osteoblasts (OsbExos) for 6 days. (One-way ANOVA. n=3–5; p-value * < 0.05; ** < 0.01; ***, P < 0.001)